Brinkmann, T.; Pohlmann, J.; Bram, M.; Zhao, L.; Tota, A.; Escalona, N.J.; de Graaff, M.; Stolten, D.:

Investigating the influence of the pressure distribution in a membrane module on the cascaded membrane system for post-combustion capture

In: International Journal of Greenhouse Gas Control (2015) Elsevier

DOI: 10.1016/j.ijggc.2015.03.010

Investigating the influence of the pressure distribution in a membrane module on the cascaded membrane system for post-combustion capture

Tosten Brinkmann [a], Jan Pohlmann [a], Martin Bram [b], Li Zhao [b,*], Akos Tota [c], Natividad Jordan Escalona[d], Marijke de Graaf, Detlef Stolten [b, f],

[a] Institute of Polymer Research, Helmholtz-Zentrum Geesthacht, Max-Planck- Str.1, D-21502, Geesthacht, Germany

[b] Institute of Energy and Climate Research, Forschungszentrum Jülich, D-52425 Jülich, Germany

[c] Linde Engineering, D-82049 Pullach, Germany

[d] RWE Power Aktiengesellschaft, D-45128 Essen, Germany

[e] EnBW Energie Baden-Württemberg AG, Durlacher Allee 93, D-76131 Karlsurhe

[f] Chair for Fuel Cells, RWTH Aachen University, D-52056 Aachen, Germany

[*]Corresponding author

Email: l.zhao@fz-juelich.de

Abstract

Polyactive® membranes shows a promising properties for CO_2 separation from flue gas. An investigation of different module types using Polyactive® Membrane was carried out in this paper. A test rig was built to explore, amongst other process parameters, the pressure drop in envelope type membrane modules. The experimental data and simulation results were compared, which shows a quite good consistent tendency. This validation enabled further simulations for different modules in a virtual pilot plant configuration. Applying the data from the pilot plant simulation for a reference power plant, the scale-up cascaded membrane system was analysed using different membrane modules. Considering the required membrane area, energy consumption and pressure drop in different modules, a counter-current membrane module configuration shows the best performance, and has a marginal advantage in comparison with the chemical absorption process.

Keywords: Carbon capture, gas separation, membrane module, pressure drop, efficiency loss, post-combustion

1. Introduction

Energy-related CO_2 emissions reached a record 31.2 gigatonnes in 2011, representing by far the largest source (around 60%) of global greenhouse-gas emissions, measured on a CO_2-equivalent basis [1]. An update info released from World Bank warns about the potentially disastrous consequences that a four degree celsius warmer world will have by 2100 [2]. Forecasts from the IEA and others show that “decarbonising” electricity and enhancing end-use efficiency can make major contributions to the fight against climate change [3], *i.e.*, in spite of increased energy efficiency, the electricity demand is projected to increase substantially, with up to 50% from today towards 2050. This demand will be supplied by a

minimum of 40% electricity generation by Renewable Energy System (RES), with the remainder being filled up with nuclear and fossils with Carbon Capture and Storage (CCS) [4]. CCS is a series of technologies and applications which enable the capture of CO_2 from large source points, its transport via pipelines and ships and its safe storage in geological formations such as saline aquifers and depleted oil and gas fields [5].

The theory of CCS is clear: keep using fossil fuels and capture and store the released CO_2 underground. However, the technology is currently still in a developing state and has to be demonstrated to be feasible on a large scale at acceptable cost. Apart from high investment costs, a high CO_2 price or regulations will be required to trigger actual use of the CCS part, as a significant share of the power is needed to drive the gas separation units, thereby lowering the plant's net efficiency and flexibility [4]. Across different regions in the world, post-, pre- and oxy-combustion CO_2 capture are considered options for large-scale demonstration of CCS from power generation. To date, no individual capture route or technology can claim a general competitive advantage over other processes [3].

The competing technologies for post-combustion carbon capture are absorption, adsorption and membrane methods [5, 6]. As the 1st generation technology for CO_2 capture amine absorption is a mature and proven purification technique that is widely employed in the industrial treatment of acid gases [7]. Nevertheless, the high energy consumption of the absorbent (mono ethanol amine, MEA) regeneration step, namely efficiency losses of 10-14 %-points and corrosion problems associated with solvent degradation increase the operation and maintenance costs of this technology [8-13]. Gas separation membrane technologies, a potential 2nd generation technology for post-combustion capture is drawing more and more attention. They show advantages in their potential for less environmental impact, and membrane modules can be used as add-on equipment with fewer modifications to power plants. The other potential advantage is that for low degrees of CO_2 separation a stage-

arranged membrane system demands a lower specific energy than that required for MEA absorption. Furthermore are membrane systems more easily scalable and more suitable for intermittent, dynamic operation. Membrane science and technology can be divided into two classes, namely material research and process engineering. Many groups and researchers in the world were involved in the material and process development [14-29], with some institutions covering the entire research and development chain from material synthesis to process engineering [21, 22, 30, 31].

Important progress and relevant experience were obtained in the past with membrane modules tested in a real flue gas environment. In Europe, under the frame work of projects MemBrain [32], METPORE [33], Nanoglowa [34] and iCap [35] different polymer and ceramic membranes are being investigated to meet the harsh requirement in coal-fired power plants [17, 21, 23, 27, 29]. Membrane modules equipped with Polyactive® Thin-Film-Composite Membranes [36-39] in a parallel configuration (12.5 m^2 and 1 m^2), are being tested in EnBW Rheinhafenkraftwerk [29, 33]. A 1 MW_{el} pilot-scale Polaris® membrane separation system at the Department of Energy's National Carbon Capture Center in Wilsonville, USA, was announced by the National Energy Technology Laboratory (NETL) in November, 2012, for the testing of a post-combustion membrane capture technology on the world's largest scale to date [22, 40].

In order to realize the potential of gas permeation for industrial applications, advanced membrane module concepts are desirable. Membranes can be inserted in three major types of modules for gas separations applications: envelope type, spiral-wound, and hollow-fiber modules [41-44]. In general the membrane module must be used in commercial processes as a package, which contains as much surface area per unit volume as possible, with good flow distribution and efficient contact of the feed gas within the membrane. The main different flow configurations in membrane gas permeation processes are cross plug flow, co-current

flow and counter-current flow [42]. More specifically, hollow-fiber modules may be designed with reasonable precision to approximate an idealized counter-current when the permeate pressure is significant, or to approximate a cross-flow pattern when the permeate pressure is low enough [41]. The most commonly used flat sheet membrane module for gas separation is the spiral-wound module, which is dominated by cross-flow [22]. Within an envelope type module, the first half of a membrane envelope can be assumed to be in co-current flow configuration, whilst the second half is in countercurrent flow configuration [37]. The packing density (PD) of each type which is regarded as the surface area per volume [m^2/m^3] is shown in Table 1. Furthermore, the flow patterns do not only influence the concentration distribution on the feed and permeate sides of the module but also give rise to different behavior of the pressure drops [42, 45] and hence the utilization of the available driving force.

Table 1 Packing density range of different membrane module forms [41]

Module form	PD [m^2/m^3]
Hollow fiber	2000~5000
Spiral wound	700~1000
Envelope module	500~900

Although hollow fibre modules appear to be superior in terms of utilisation of membrane area, they have substantial drawback when high flux membrane materials in a thin film composite configuration are to be employed. In order to transfer the attractive CO_2/N_2 selectivities of ca. 60 at 20°C of poly ethylene oxide block copolymers as Polyactive® or Pebax® 1657 [36, 46] into a membrane module whilst also achieving high CO_2 permeances in

the order of 3 $Nm^3/(m^2\,h\,bar)$ at 20°C, ultrathin layers in the order of 70 nm thickness are required. This ambitious goal can be met in the manufacture of flat sheet membranes in a 100 m^2 scale [38]. To the authors' knowledge, no comparable coating technology is available for hollow fibre membranes. In the present work, different flow patterns of flat sheet membrane modules will be investigated under the framework of METPORE II project [33, 37]. The envelope type modules used in the experiments were developed by Helmholtz-Zentrum Geesthacht (HZG) [37, 43, 47], which were tested both in a pilot plant-scale and in the flue gas of the power plant Rheinhafendampfkraftwerk (EnBW). The pressure drop in the modules was investigated. The relevant results were integrated with a total system analysis, using the flue gas data of the Reference Power Plant North Rhine-Westphalia (RKW-NRW) [48] and power plants Rheinhafendampfkraftwerk (EnBW) and Niederaußem (RWE). The equation oriented process simulator Aspen Custom Modeller® [49] was used for membrane module simulation. The cascaded membrane process was investigated by Aspen Process Modelling V8.0.

2. Investigation of pressure distribution in a flat sheet membrane module [37]

2.1. Introduction of membrane material and module

The membrane considered in this study is a multilayer, thin film composite membrane specifically developed for the separation of CO_2 from N_2. Details on this membrane can be found in [36-39, 50]. The 70 nm thin separation layer consists of the polyethylene/ polybutylteraphtalate blockcopolymer Polyactive®. The active layer is sandwiched inbetween two highly permeable polydimethylsiloxane layers cast in turn onto porous support structure consisting of polyacrylo nitrile and polyester. The CO_2 permeance and the CO_2/N_2 selctivity of this membrane is similar to the values published for the MTR Polaris® membrane [51]. It has been extensively tested for applications as diverse as biogas processing [38, 39], separation of CO_2 from reaction products [52, 53] and flue gas treatment [37, 38]. The

relevant permeation properties are given in Table 2. Only CO_2, N_2 and O_2 are listed. The permeance of Ar is assumed to be identical to that of O_2 whilst that of CO_2 is assumed to be ten times the value of that for CO_2. The parameters given are that for the Free-Volume model [37, 54, 55] that has been employed to express multicomponent permeation behaviour in modelling. The parameters were determined using single gas measurements employing the pressure increase method. The membrane can be produced in 100 m^2 scale and was installed in different module types, mostly into envelope type modules.

Table 2. Free-Volume parameters for Polyactive® composite membrane [37]

	L^0_∞ [$Nm^3/(m^2\ h\ bar)$]	E [kJ/kmol]	m_0 [1/bar]	m_T [1/K]	σ [Å]
CO_2	1084.66	14279.81	0.1568	-0.0054	3.941
N_2	68646.60	34251.30	0.0000	0.0000	3.798
O_2	39776.50	30463.00	0.0000	0.0000	3.467

These modules have a maximum capacity of 75 m^2 with a length of 1250 mm and a diameter of 310 mm, depending on envelope thickness. The membrane material is manufactured into membrane envelopes consisting of two sheets of membrane material with their separation layer on the outside, permeate spacer inbetween the sheets and thermally welded at the outer circumference. The permeate is withdrawn radially towards a central hole. The membrane envelopes are stacked on a perforated permeate tube and subdivided into compartments, thus allowing for an adjustment of crosssectional area according to the amount of permeate withdrawn. Hence a nearly constant flow verlocity on the feed side can be realised. More details on this module type can be found in [37, 44, 47]. The spiral wound membrane module is widely used in membrane technology, its design features are outlined in [43]. A novel concept for flat sheet membranes is closely related to the envelope type [23, 37, 38]. However, the envelopes are rectangular and supposed to be housed in a module with a rectangular cross section. The design allows for different location of permeate withdrawal so

that different flow patterns can be realised, *i.e.* co- and counter- current design. Furthermore, it is possible to divide the envelope into segments, thus realising different permeate withdrawal points along the flowpath from feed to retentate and hence minimising the permeate side pressure drop. Figure 1 illustrates the investigated module types.

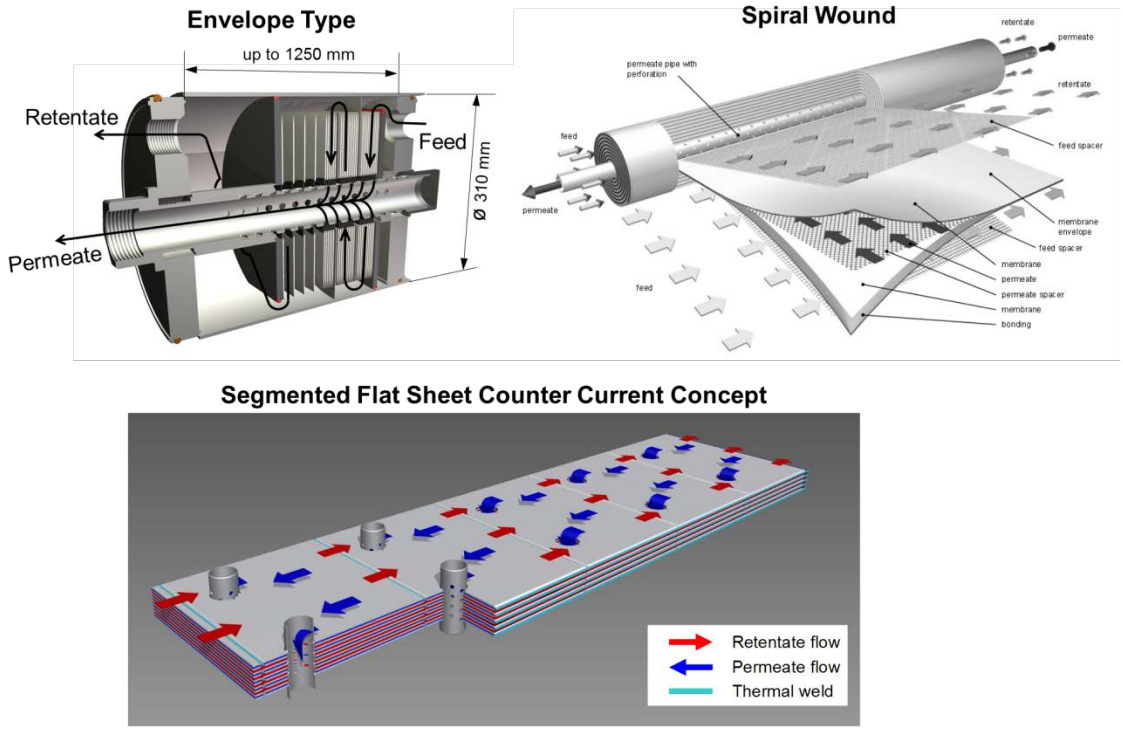

Figure 1: Types of investigated membrane modules

2.2. Test equipment

The envelope type module was extensively studied in pilot plant investigations for the separation of CO_2 from various gas streams using Polyactive® membranes [23, 37-39] and is employed in numerous industrial applications in the chemical and petrochemical industries [44, 47, 56]. The analysis of different module types presented in [37] constrained itself to two applications. Next to synthetic gas mixtures, also a bypass stream of the

Rheinhafendapfkraftwerk was supplied to a dedicated pilot plant within the scope of the project METPORE II, funded by the German Minstry of Economics and Energy. A simplified flowsheet is shown in Figure 2. A separate publication describing its design and the achieved results in detail is in preparation [57].

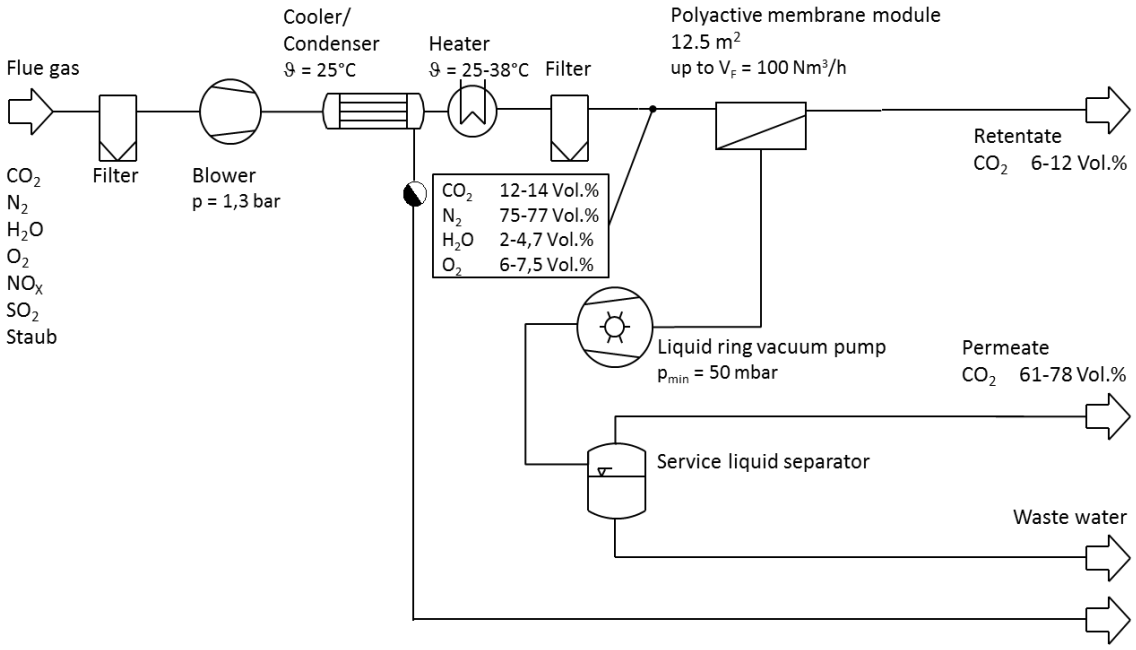

Figure 2. Gas permeation pilot plant for power plant flue gas, installed at EnBW Rheinhafendampfkraftwerk, Karlsruhe, Germany

2.3. Modelling validation

The permeation behavior of multicomponent mixtures through Polyactive® multilayer composite membranes can be described by the Free-Volume model using the parameters given in Table 2. In [37, 45] it was shown that the combination of this model with an appropriate model describing the membrane module flow patterns can very accurately predict the separation performance of envelope type modules. It is assumed that this is also true for the other membrane module types considered, whilst it has to be emphasized that an experimental proof for this is currently under investigation. The details of the employed

models can also be found in [37]. They were implemented in the equation oriented process simulator Aspen Custom Modeler (ACM) [49]. The operating conditions investigated in the pilot plant as well as the experimental and simulation results for the retentate pressure are summarised in Table 3. It is apparent that the simulation results closely reflect the experimental values. The prediction of the separation performance is equally good [37]. The relevant results for pressure drop investigations employing real flue gas at the EnBW Rheinhafendampfkraftwerk are shown in Table 4. The accuracy of the model predictions allows the application of the developed models for the estimation of the required compression energies.

Table 3. Experimental conditions of the pilot plant experiments using synthetic gas mixtures and experimentally determined as well as simulated retentate pressures at a temperature of 20°C for an envelope type membrane module containing 9.52 m^2 of Polyactive® membrane [37]

Experiment no.	Feed volumetric flowrate [Nm^3/h]	Feed pressure [bar]	Permeate pressure [bar]	Feed CO_2 mole fraction [-]	Retentate Pressure [bar]	
					Experiment	Simulation
1	43.64	4.41	0.20087	0.181	4.34	4.33
2	44.41	4.48	0.111	0.177	4.41	4.40
3	36.00	4.38	0.099	0.180	4.33	4.32
4	26.31	4.32	0.095	0.182	4.29	4.28
5	34.24	2.55	0.201	0.174	2.45	2.45
6	33.64	2.49	0.100	0.176	2.40	2.39
7	20.07	2.52	0.101	0.182	2.48	2.48
8	42.61	4.44	0.200	0.167	4.36	4.36

Table 4: Experimental conditions of the pilot plant experiments using flue gas and experimentally determined as well as simulated retentate pressures at temperatures of 24 to 28°C for an envelope type membrane module containing 12.5 m^2 of Polyactive® membrane

Experiment no.	Feed volumetric flowrate [Nm^3/h]	Feed pressure [bar]	Permeate pressure [bar]	Feed CO_2 mole fraction [-]	Retentate Pressure [bar]	
					Experiment	Simulation
1	50.00	1.13	0.060	0.135	1.10	1.09
2	50.30	1.14	0.062	0.130	1.11	1.11
3	60.20	1.18	0.063	0.135	1.14	1.13
4	69.90	1.24	0.057	0.135	1.19	1.19
5	80.00	1.31	0.062	0.129	1.25	1.25
6	50.30	1.14	0.075	0.129	1.11	1.11
7	59.70	1.19	0.066	0.131	1.15	1.15
8	65.00	1.22	0.075	0.128	1.18	1.17
9	69.60	1.23	0.065	0.136	1.18	1.18
10	70.40	1.25	0.069	0.129	1.20	1.19
11	79.60	1.29	0.067	0.138	1.22	1.23
12	80.10	1.31	0.069	0.130	1.25	1.25
13	80.10	1.31	0.069	0.135	1.25	1.25
14	80.30	1.30	0.067	0.136	1.24	1.24
15	80.60	1.31	0.069	0.136	1.25	1.25
16	60.30	1.20	0.111	0.128	1.16	1.15
17	79.70	1.32	0.116	0.129	1.25	1.26
18	80.00	1.31	0.100	0.137	1.25	1.25
19	80.30	1.32	0.100	0.132	1.25	1.26
20	60.00	1.20	0.150	0.128	1.16	1.16
21	70.00	1.26	0.151	0.131	1.20	1.21
22	80.00	1.32	0.150	0.128	1.26	1.26

2.4. Simulation of different module types in a virtual pilot plant configuration

Figure 3 illustrates a possible pilot plant system. A feed flow of 1000 Nm^3/h was assumed to enable the investigation of membrane module types commonly employed in today's gas permeation installations. The blower C1 is used to compensate the pressure drops of the membrane modules installed in the first stage of the process, *i.e.* the retentate pressure is set to atmospheric pressure and the outlet pressure of C1 is adjusted according to the pressure drop. The simulation assumed an adiabatic compression with an efficiency of 70%. The heat exchanger combination H1 and H2 is used to cool the feed gas to 25°C and to separate condensed water whilst H2 is increasing the feed temperature above the dew point in order to prevent condensation in the downstream system. The membrane modules in MemStage1 are separating CO_2 from the feed gas according to the set recovery target, i.e. the degree of CO_2

separation, which was assumed to be 50% for this investigation. The vacuum pump C2 is compressing the permeate of the first stage. Its suction pressure is set to 100 mbar. Since water is preferentially permeating the membrane, i.e. even more strongly than CO_2, the separator S1 is employed to draw of the liquid water. The vacuum pump is assumed to operate isothermal with an efficiency of 40%, as can be realised by liquid ring vacuum pumps. In operation, this lower efficiency is offset by a simple, robust design, the partial condensation of permeated water in the service liquid circuit and a lower demand of cooling utilities since the heat of compression is transferred into the service liquid which can be cooled down in a straightforward fashion. The adiabatic compressor C3 is increasing the pressure to 6 bar, *i.e.* the operating pressure of the second stage, at an efficiency of 70%. The heat exchanger H3 is cooling down the gas and removing the liquefied water. The membrane stage MemStage2 is employed to further increase the CO_2 concentration of the permeate stream of MemStage1 to the required purity, *i.e.* 95 Vol.-%, in the permeate of the second membrane stage at a pressure of 1.0130 bar. In order to meet the required recovery, the retentate is recycled upstream of H1. Part of the compression energy is recovered by the turbo expander T1 (efficiency 70%).

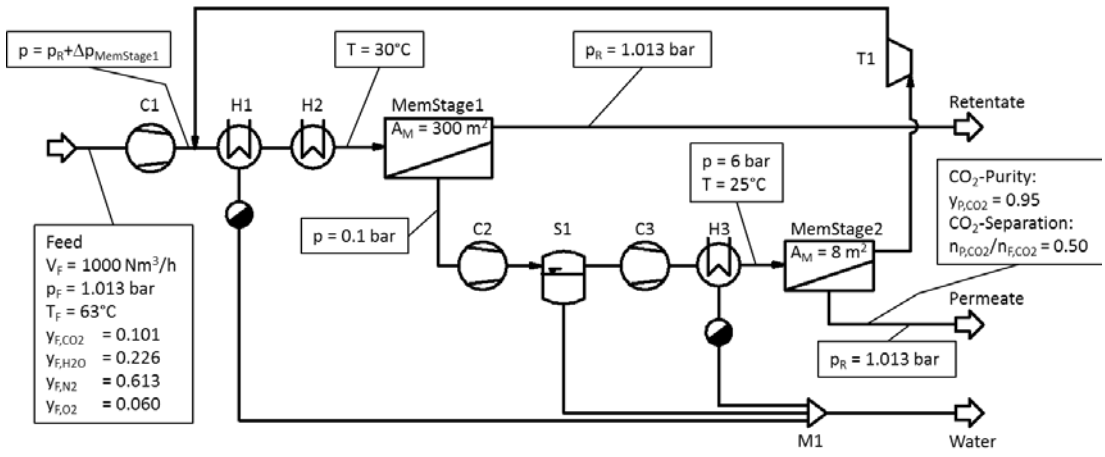

Figure 3. Pilot plant flow sheet

As a comparison case, the required membrane areas were calculated for the described separation task (i.e. a CO_2 purity of 95 Vol.-% at a degree of CO_2 separation of 50 %), assuming the membrane stages can be described as cross flow stages with unhindered permeate withdrawal and no pressure drops on feed and permeate sides as well as no concentration polarisation. The dependency of the permeances on temperature, pressure and composition as well as real gas behaviour for the calculation of the driving forces and non-isothermal operation due to the Joule-Thomson effect were considered. The latter two phenomena are of minor effect, especially in the first stage, due to the low pressures and the small stage cut. The simulation rendered area requirements of 300 m^2 for stage 1 and 8.2 m^2 for stage 2. Using these area requirements, flat sheet membrane modules were dimensioned for the two stages. The following module types were considered, see also Figure 1:

- Envelope type membrane module.
- Spiral wound membrane module.
- Counter current membrane module concept with one segment. The permeate is led counter currently to the feed flow and is withdrawn at the feed side of the module.
- Co current membrane module concept with one segment where the permeate is withdrawn co-currently with the feed at the retentate location.
- Counter current membrane module concept with four segments. The module is divided into four section of equal length at the start of each permeate is withdrawn at the location of the feed.

Next to the already described phenomena, pressure drops on feed and permeate sides as well as concentration polarisation on the feed side were considered. Details on the simulation models employed, their implementation into Aspen Custom Modeler® [49] and the employed geometrical values can be found elsewhere [37]. Tables 5 and 6 show the module details required for the simulation for stages 1 and 2, respectively. All membrane modules are

assumed to be equipped with Polyactive® membrane [36-38]. For the co- and counter- current membrane module concepts, one membrane module can be used for each of the stages, since this concept is quite versatile in terms of adjusting it for different flow rates. However, an important point to mention is that the simulation predictions for this module type have not been validated experimentally yet. For the envelope type and spiral wound modules it is assumed that five or eight modules are mounted in parallel in the first stage, respectively. In case of the spiral wound modules, a second sequential set of seven parallel modules is required to realise the required membrane area. For the second stage, one membrane module is sufficient for both, the envelope and the spiral wound module types.

Table 5. Membrane module details stage 1

	Envelope	Spiral wound	Counter-current	Co-current	Counter-current 4 segments
Membrane area per module A [m^2]	60.21	20.11	300.72	300.72	300.72
Number of modules in parallel	5	8 and 7	1	1	1
Module diameter D [m]	0.310	0.203	-	-	-
Number of envelopes	506	11	127	127	127
Compartments	9	-	-	-	-
Envelope breadth b [m]	-	0.914	0.600	0.600	0.600
Envelope length l [m]	-	1.000	1.973	1.973	4 x 0.493
Feed channel height h_R [mm]	1.500	1.500	1.500	1.500	1.500
Permeate channel height h_P [mm]	1.500	1.500	1.500	1.500	1.500

Table 6. Membrane module details stage2

	Envelope	Spiral wound	Counter-current	Co-current	Counter-current 4 segments
Membrane area A [m^2]	8.33	8.33	8.21	8.21	8.21
Number of modules in parallel	1	1	1	1	1
Module diameter D [m]	0.310	0.159	-	-	-
Number of envelopes	70	9	5	5	5
Compartments	22	-	-	-	-
Envelope breadth b [m]	-	0.693	0.300	0.300	0.300
Envelope length l [m]	-	0.668	2.736	2.736	4 x 0.684
Feed channel height h_R [mm]	1.500	1.500	1.500	1.500	1.500
Permeate channel height h_P [mm]	1.500	1.500	1.500	1.500	1.500

The results of the simulations are summarised in Table 7 and Figures 4, 5 and 6. Since stage 1 governs the process, the discussion will focus on this stage. The differences in pressure drops for the investigated modules are rather small, as shown in Figure 4. It is apparent, that both, the non-segmented counter current and the co current modules have the highest permeate side pressure drops and low feed side pressure drops. The latter is also true for the four segment counter current concept. However, due to the segmentation, low permeate side pressure drops can be realised. This also causes a superior pressure ratio (Figure 5) and a good CO_2 driving force (Figure 6). The permeate side pressure of the spiral wound modules is quite high. This is due to the long permeate pathways. High pressure drops also cause the high feed side pressures. In combination, this translates in a good pressure ratio and a good driving force (Figures 5 and 6). The fluid dynamically best performing module is the envelope type module. It has very short permeate pathways resulting in small permeate side pressure drops (Figure 4). Using the calculated performance data for the different modules to compare CO_2 purities and recoveries as well as the required power for the blower C1, the vacuum pump C2 and the compressor C3, it is apparent that the segmented counter current module renders the highest CO_2 purity at the highest recovery with the envelope type and the spiral wound modules being close contenders. Considering the one segment co- or counter-current modules, the situation regarding CO_2 recovery is more pronounced: a strong decrease of recovery, especially for the co- current module can be observed. This is due to the inferior pressure ratio and driving force distribution in these module types (Figures 5 and 6). In terms of compression power consumption, the highest demand is caused by the vacuum pump C2 followed by the compressor C3 and the blower C1. The lowest power demand for the vacuum pump can be found for the co-current module since this module has the lowest permeate flow rate due to its inferior driving force utilisation, *i.e.* the vacuum pump power follows the permeate flow rate to be withdrawn from stage 1. The power demand of the compressor C3

has a similar behaviour since it is employed to recompress the permeate of stage 1 for feeding it to stage 2. Since envelope type and spiral wound modules have the highest feed side pressure drops of the considered cases¸ the blower powers are higher for these modules with the consumption for the spiral wound being the highest. This is caused by the high velocity on the feed side, i.e. 2.5 m/s, compared to ca. 2 m/s for the other cases. This high velocity resulted from distributing modules of a given area and geometry to achieve the required membrane area.

It can be concluded that the segmented counter current membrane module appears to be the best choice in terms of CO_2 purity and recovery as well as energy consumption for the rotating equipment.

Table 7. Simulation results

	Envelope Type	Spiral Wound	Counter-Current 1 Segment	Co-Current	Counter-Current 4 Segments
CO_2-Purity [kmol/kmol]	0.944	0.943	0.946	0.932	0.945
CO_2-Recovery [-]	0.451	0.451	0.431	0.401	0.455
Membrane Area Stage 1 [m^2]	301.070	301.620	300.716	300.716	300.716
Membrane Area Stage 2 [m^2]	8.330	8.330	8.207	8.207	8.207
Total Membrane Area [m^2]	309.400	309.950	308.923	308.923	308.923
Power Blower C1 [kW]	7.991	9.260	7.260	7.296	7.262
Power Vacuum Pump C2 [kW]	17.674	17.875	17.782	15.902	17.751
Power Compressor C3 [kW]	9.016	9.177	8.769	8.320	8.940
Power Turbine T1 [kW]	-0.933	-0.985	-0.952	-0.928	-0.927
Total Power [kW]	33.748	35.326	32.859	30.592	33.026
Total Cooling Duty [kW]	-137.607	-139.318	-136.351	-135.971	-136.623
Pressure Drop Stage 1 retentate [bar]	0.092	0.120	0.076	0.077	0.076
Max.Pressure Drop Stage 1 permeate [bar]	0.0002	0.0088	0.0118	0.0152	0.0008
Pressure Drop stage 2 retentate [bar]	0.340	0.005	0.088	0.084	0.089
Max. Pressure Drop Stage 2 permeate [bar]	0.0015	0.0318	0.1638	0.2545	0.0152
Permeate Flowrate Stage 1 [Nm^3/h]	97.901	98.990	98.500	88.040	98.300

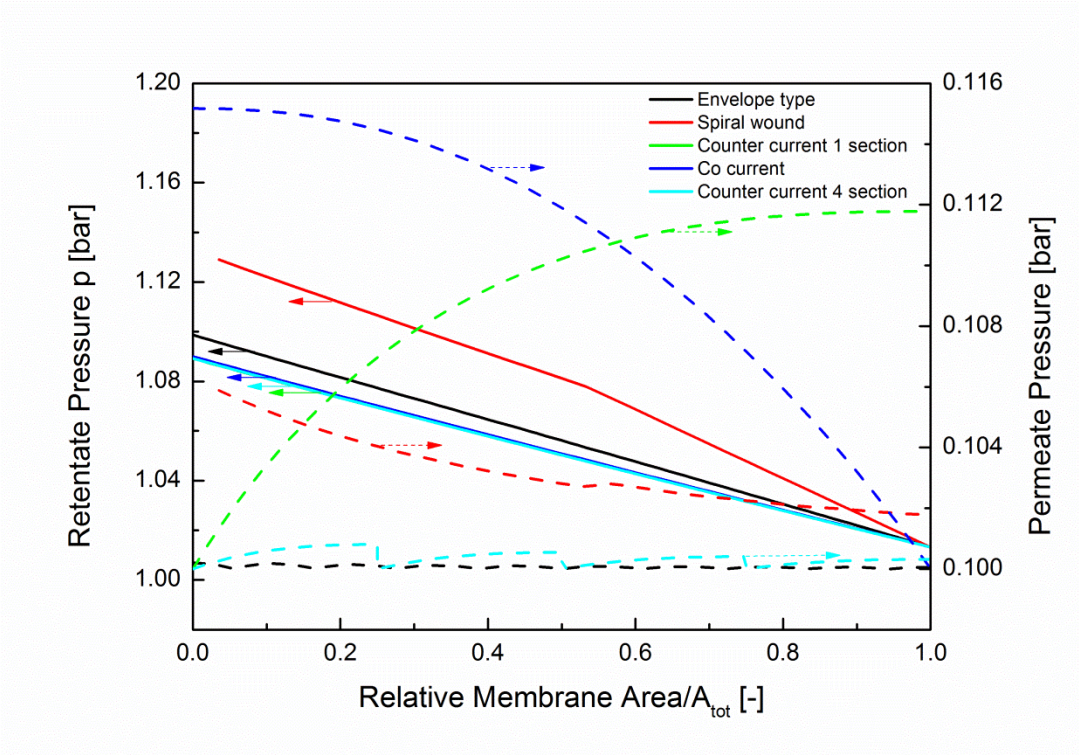

Figure 4. Retentate/feed side and permeate side pressures of the different module types

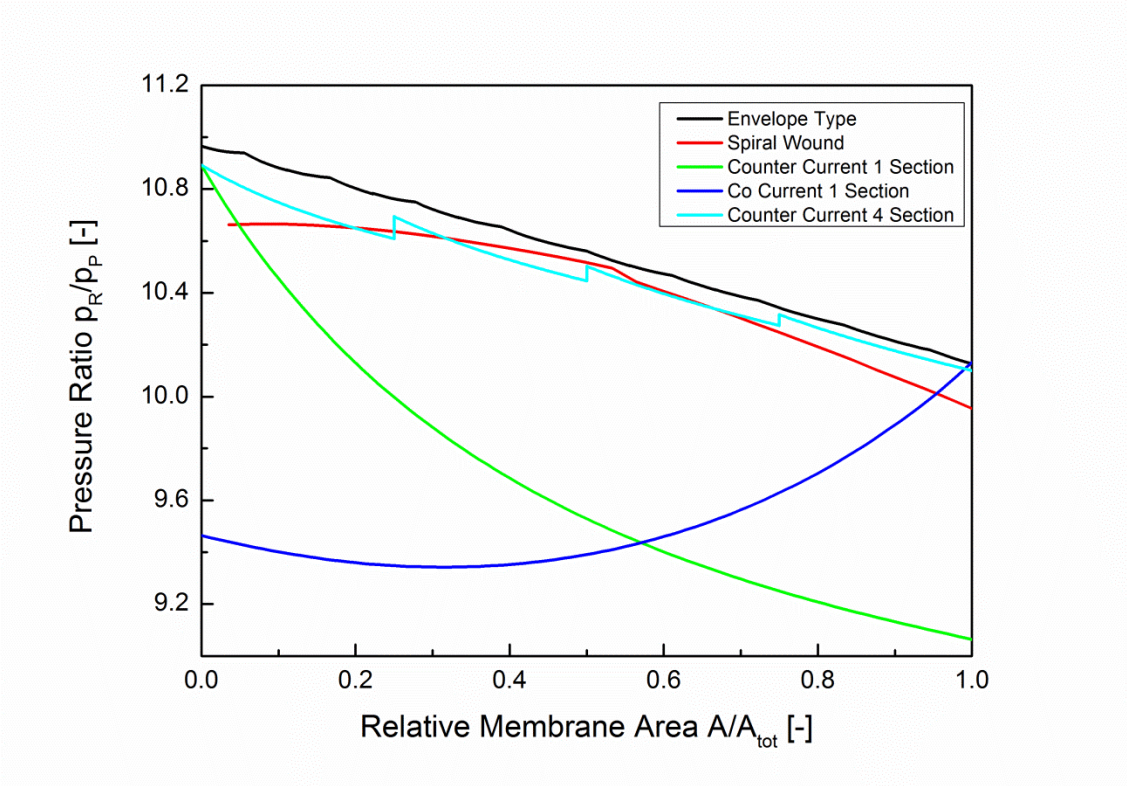

Figure 5. Pressure ratios of the different module types

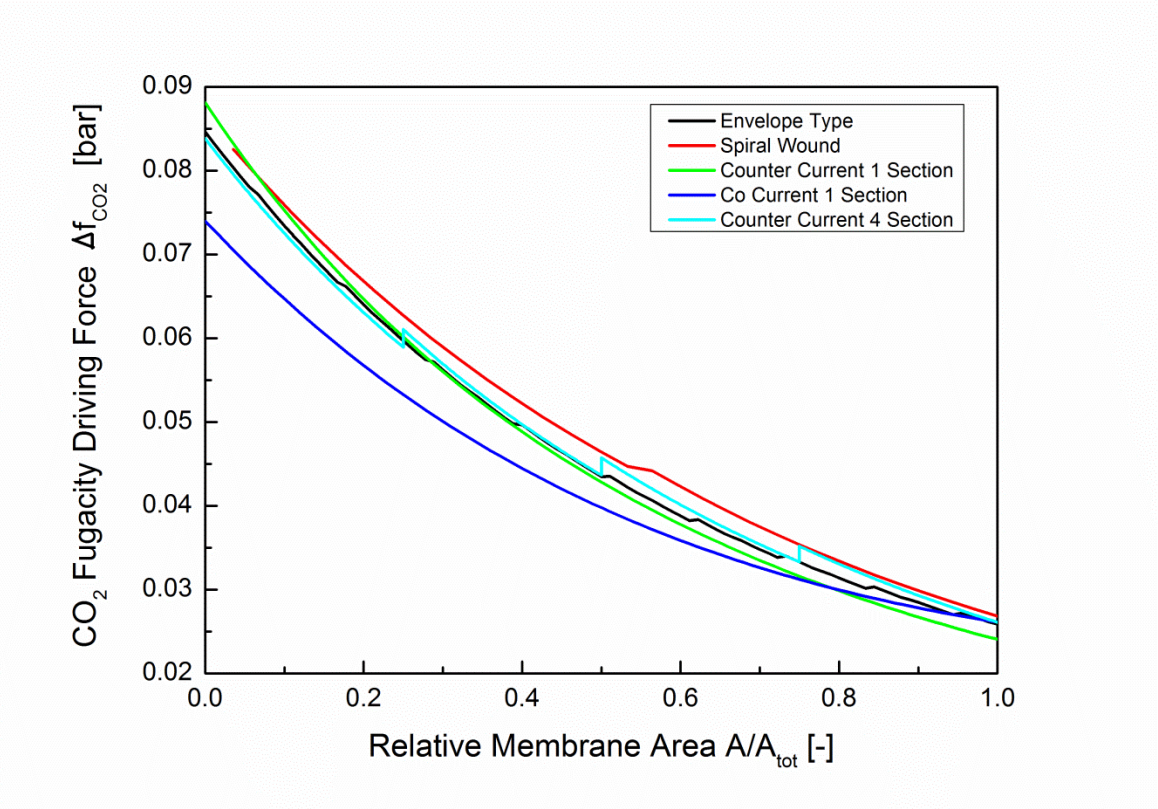

Figure 6. CO_2 driving forces of the different module types

3. Power plants data used for simulation

A scale-up cascaded membrane system, shown in Figure 7, was used for the process analysis. The first membrane (Mem 1) is driven by a combination of a blower and avacuum pump and the second membrane (Mem 2) only by compressor. The retentate of the second membrane is recycled to the feed of the first membrane. Part of the compression energy is recovered by a turbo expander. The membrane cascade is located downstream of the SCR-DeNOx, dust removal (E-filter) and desulphurization (FGD) processes and prior to the cooling tower. Here the flue gas has a pressure of approximate 1 atm and a temperature of 50~70°C. The basic data of RKW-NRW and the flue gas data are listed in Table 7. The flue gas data were obtained by simulation using Klein Kopje hard coal. The residue of the pollutant in the flue gas consists of approximately 50 vppm SO_2 and approximately 200 vppm NO_2.

The temperature, H_2O permeance and relative humidity have an evident influence on CO_2 selective process of the polymer membranes [58]. In order to develop feasible membrane system, these influence factors must be considered.

A wet scrubber was adopted in the upstream of the membrane system, referring to a post-combustion process presented by RWE [59]. There are two functions of this scrubber, the one is the pollutant (SOx, NOx and dust) of flue gas can be further reduced, e.g. SOx can be decreased to 10 vppm; the other is the flue gas can be further cooled down to 25~30°C. The latter is a crucial factor for the membrane process, because the working temperature of the Polyactive® membrane influences its performance strongly [60]. Furthermore, applying dewatering process prior to CO_2 separation leads to a lower energy consumption of the whole system [60]. Here, 2/3 water content of the flue gas is removed.

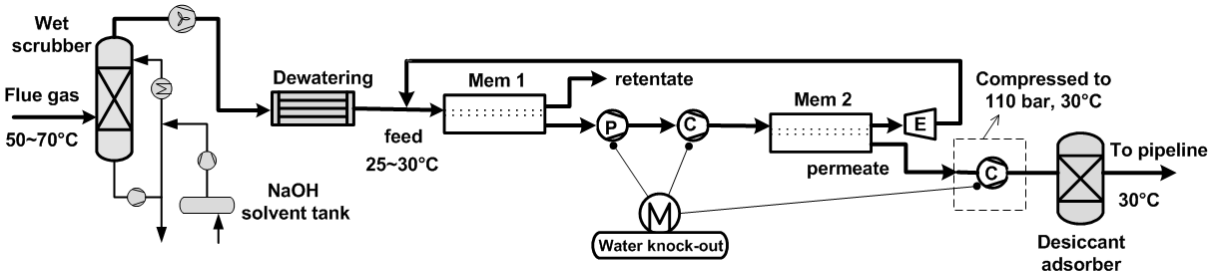

Figure 7. Schematic illustration of the scale-up cascaded membrane system

Table 8. RKW-NRW power plant basic data and simulation results of the flue gas conditions after removal of the pollutants using Klein Kopje hard coal [60]

Power plant RKW-NRW		
Output gross	600	MW
Output net	555	MW
Net efficiency	45.9	%
Steam parameters	285	bar/ 600°C / 620°C
Operating time	8000	h/year
Fuel input	1.33	Mt/year
Investment costs	534.4	million euro
O & M costs	7.8	million euro/year
Fuel costs	72.8	euro/t
Electricity price	4.355	cent/kWh
Flue gas conditions after removal of the pollutants		
Pressure	1.05	bar
Temperature	50	°C
Flow rate	1.6	million Nm^3/h
Main components		
CO_2	13.5	mol%*
N_2	70.1	mol%*
O_2	3.7	mol%*
H_2O	11.9	mol%*
Ar	0.8	mol%*

* simulated

4. Integrating the module data with the scale-up cascaded membrane system

4.1. Simulation of single-stage system

In order to investigate the influence of flow patterns on membrane separation performance a case study was carried out. With the feed flow rate of 100 kmol/h, composition of 14.91 mol.% CO_2, 0.59 mol.% H_2O and 84.50 mol.% N_2, membrane CO_2 permeance of 3 $Nm^3/(m^2$ h bar), CO_2/N_2 selectivity of 50, H_2O permeance of 30 $Nm^3/(m^2$ h bar), two different cases were explored: for case 1, feed pressure 4 bar, permeate pressure 0.1 bar; for case 2, feed pressure 1 bar, permeate pressure 0.1 bar. The results are shown in Figure 8a.) and 8b.), respectively. The working temperature of the membranes is 25°C.

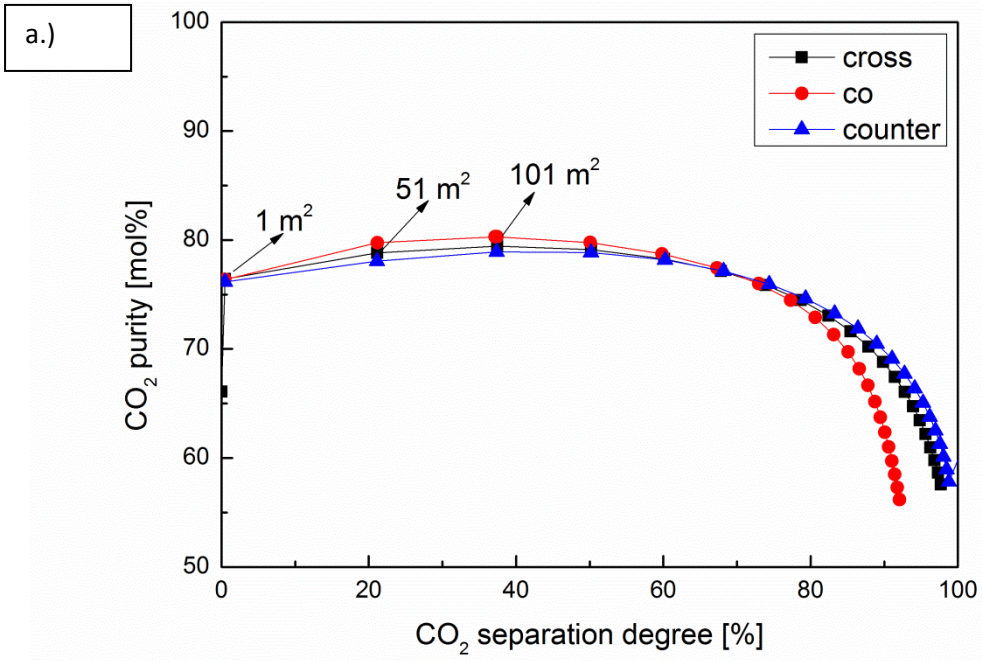

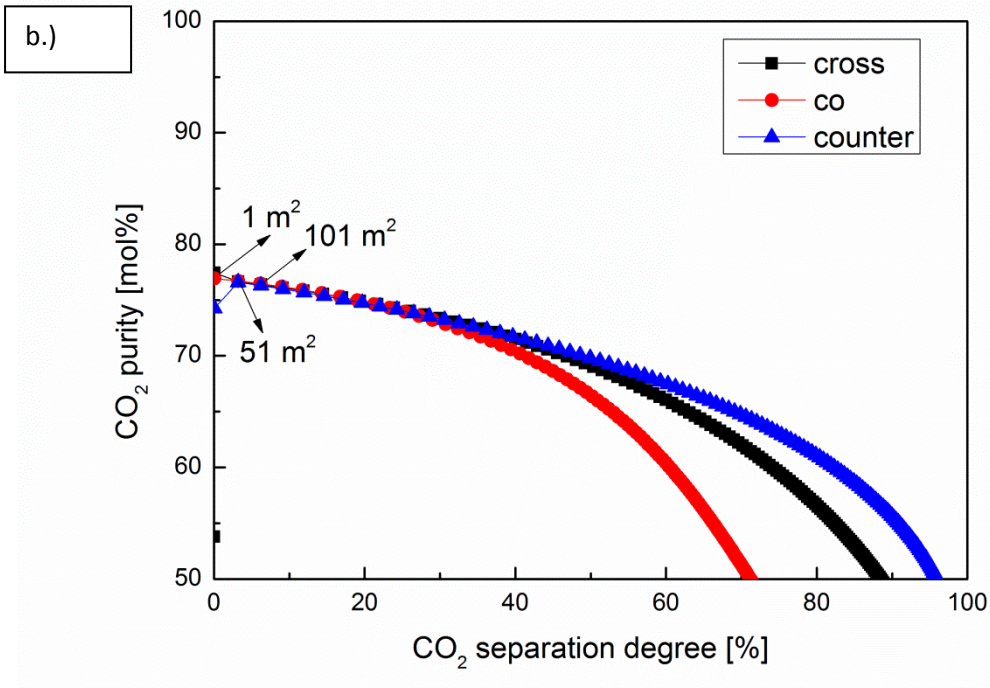

Figure 8. Polyactive® membrane performance by different flow patterns, a.) feed pressure 4 bar, permeante pressure 0.1 bar, membrane area = 1, 51, 101, 1000 m^2; b.) feed pressure 1 bar, permeante pressure 0.1 bar, membrane area = 1, 51, 101, 10000 m^2.

Comparing these two diagrams it is apparent that using both compressor and vacuum pump for a membrane leads to a smaller membrane area. For case 1, co-current flow has a little better CO_2 purity than cross- and counter-flow at a low degree of CO_2 separation (< 60%). For case 2, the CO_2 purity attenuates intensely when the degree of CO_2 separation is larger than 40%; co-current flow shows a strong decrease of CO_2 purity when the degree of CO_2 separation is larger than 40%, because of the decrease CO_2 driving force, caused by the simultaneous decrease of CO_2 content on the feed and increase on the permeate side.

4.2. Simulation of the scale-up cascaded system

Using the system shown in Figure 7, three flow patterns are investigated in the platform of NRW-reference power plant. A detailed description of the system can be found in our previous paper [61]. The feed flue gas composition and condition are listed in Table 8. O_2/N_2 and Ar/N_2 selectivity are assumed 2.8. The captured CO_2 is compressed to 110 bar of 30°C. In the study the Peng Robinson cubic equation of state with the Boston-Mathias alpha function (PR-BM) is applied as implemented in Aspen Process Engineering. The polytropic efficiency of the compressors, expanders and vacuum pumps is assumed to be 85%. 2-stage vacuum pump for Mem 1, 2-stage compressor for Mem 2 and 8-stage compressor for CO_2 compression process are used in the simulation. 30 mbar pressure drop in each intercooler is considered. The simulation results of the three different flow patterns are presented in Table 10.

The separation target of the system is defined as 95.0 mol% CO_2 purity after CO_2 compression, 50.0% and 70.0 % degree of CO_2 separation, H_2O content of 500 vppm. The optimization target of the system is the minimum energy consumption. Membrane areas of Mem 1 and 2 are the two variables, which are regulated in the simulation to reach the desired separation target.

For 50% degree of CO_2 separation, it runs smoothly to reach the aforementioned separation target. The results in Table 9 indicate that the counter current module consumes the least specific energy of 213.2 kWh/$t_{separated\ CO2}$ with the efficiency loss of 3.7%-pts.

For 70% degree of CO_2 separation, it is not problematic for cross and counter-current flow to reach the defined separation target. But for the co-current module, the program cannot converge, i.e. the co-current cascaded system cannot reach 95 mol% CO_2 purity and 70% degree of CO_2 separation simultaneously. It is well known that the Mem 1 dominates the whole separation performance of the system on the degree of CO_2 separation [61, 62]. With the help of Figure 8b.) it can be known that for a co-current module 70% degree of CO_2 separation is approaching its upper limit. This leads to the convergence problem of the system. Hence, for the co-current module, a specification design is carried out, i.e., membrane areas of the two membranes are given as input; the CO_2 purity and degree of CO_2 separation are calculated. Using the membrane areas data of cross and counter-current flows at 70% degree of CO_2 separation, the results are demonstrated in Table 10.

One point to be highlighted here is that using real flue gas for the scale-up cascaded system leads to a lower energy consumption and less membrane areas in comparison with the system using ideal flue gas (14 mol% CO_2 and 86 mol% N_2) [63]. The reason is that H_2O functions as a sweep gas, since it more readily permeates compared to CO_2. This sweep effect contributes to a lower area requirement and a less specific energy. Furthermore, counter-current flow shows the best performance both considering energy consumption and membrane area requirement.

Table 9. Influence of flow patterns on the scale-up cascaded system

Flow patterns	CO_2 purity [mol%]	Degree of CO_2 separation [%]	Membrane area [km^2]		Specific energy consumption [$kWh/t_{separated\ CO2}$]	Efficiency loss [%-pts.]
			Mem 1	Mem 2		
Cross	95.0	70.0	1.83	0.05	243.8	5.9
	95.0	50.0	0.85	0.04	217.3	3.8
Co-current	93.8	60.0	1.83	0.05	254.8	5.3
	95.2	55.3	1.52	0.05	243.5	4.8
	95.0	50.0	1.04	0.04	229.1	4.0
Counter-current	95.0	70.0	1.52	0.05	229.5	5.6
	95.0	50.0	0.79	0.04	213.2	3.7

4.3. Influence of pressure drop in membrane module on the total system energetic consumption

In order to compensate the pressure drop in membrane module additional compression energy is applied. The simulation results for three flow patterns are listed in Table 10. Furthermore, the required additional energy both at the retentate and permeate side is calculated for 50% degree of CO_2 separation, represented by a bar chart in Figure 9.

Table 10. Integrating the pressure drop of different modules with the scale-up cascaded membrane system

Module type	Degree of CO_2 separation [%]	CO_2 purity [mol%]	Pressure drop at Mem 1 retentate side [bar]	Pressure drop at Mem 1 permeate side [bar]	Pressure drop at Mem2 retentate side [bar]	Pressure drop at Mem 1 permeate side [bar]	Additional specific energy consumption [$kWh/t_{separated\ CO2}$]	Additional efficiency loss [%-pts.]
Cross	70.0	95.0	0.12	0.0088	0.005	0.0318	26.0	0.63
	50.0	95.0	0.12	0.0088	0.005	0.0318	32.4	0.56
Co-current	60.0	93.8	0.077	0.0152	0.084	0.2545	28.3	0.59
	50.0	95.0	0.077	0.0152	0.084	0.2545	29.5	0.51
Counter-current	70.0	95.0	0.076	0.0118	0.088	0.1638	21.5	0.52
	50.0	95.0	0.076	0.0118	0.088	0.1638	25.6	0.45

It is known from the results that the least additional specific energy is needed for counter-current module, owing to the lower pressure drop at retentate side. The pressure drop at the retentate side in the 1st membrane dominates the whole compression energy. In the virtual pilot plant configuration investigations of Section 2.4, the vacuum pump power demand

played a more pronounced role due of the assumption of low efficiency typical for liquid ring machines.

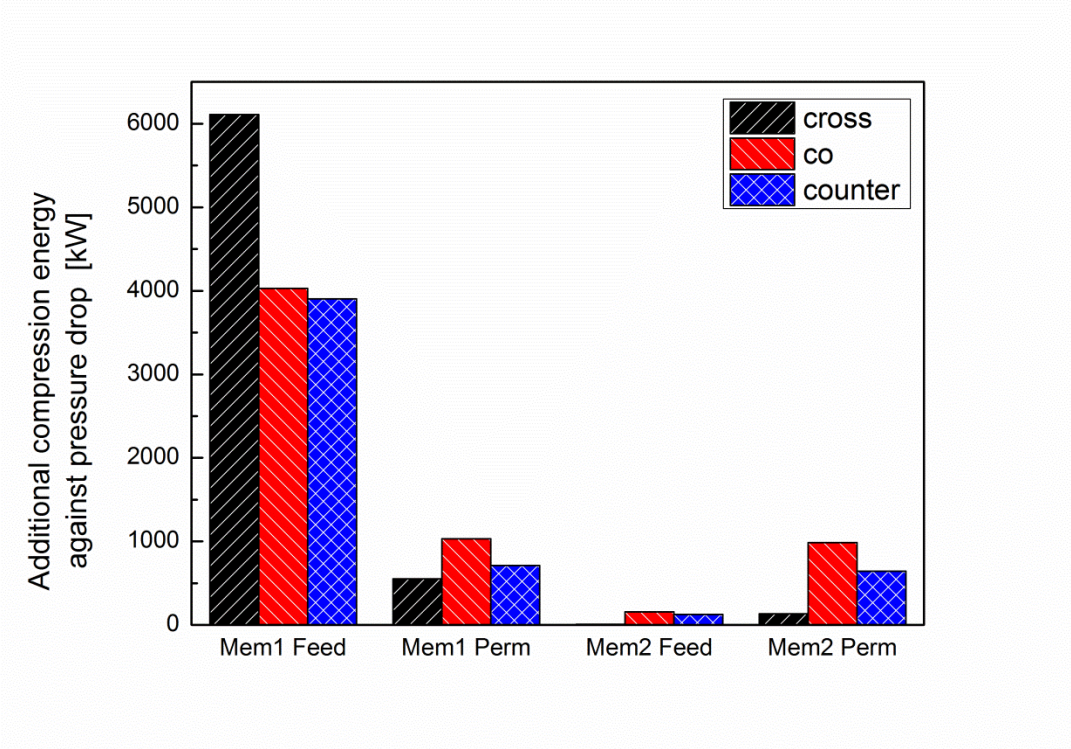

Figure 9. Additional compression energy against pressure drop in different membrane modules, at 50% degree of CO_2 separation

4.4. Comparison with chemical absorption

A comparison between membrane capture and chemical absorption is made and depicted in Figure 10. Hollow square, circle and triangle with solid line represents cross, co-current and counter current flow, respectively. When considering pressure drop (pd) in these modules, the curves are indicated by crossed symbol and dash line.

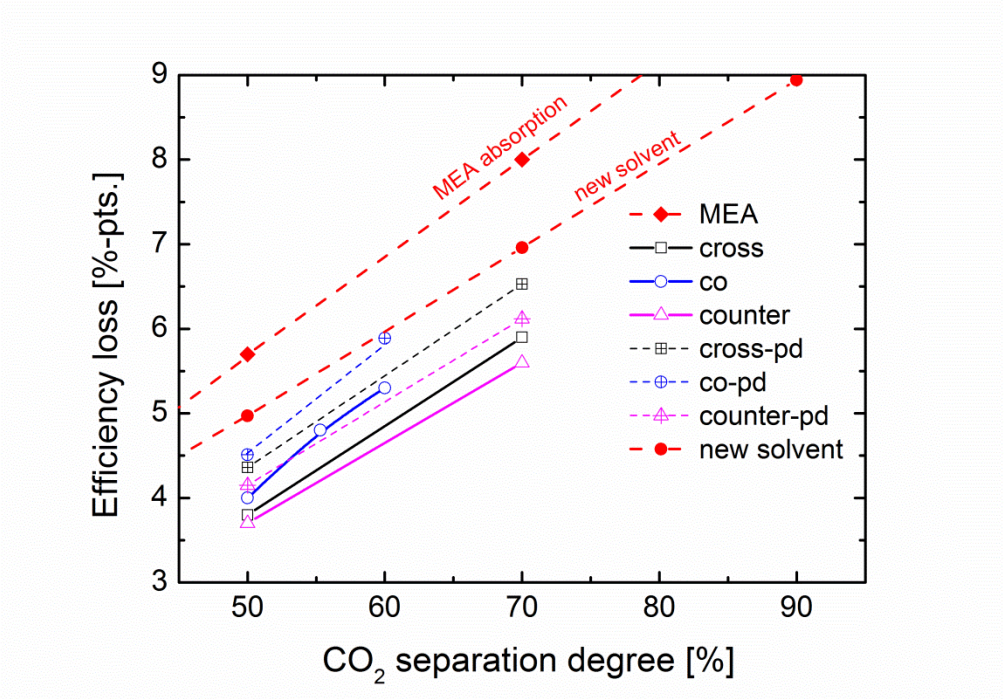

Figure 10. Comparison of efficiency loss for different flow patterns with chemical absorption

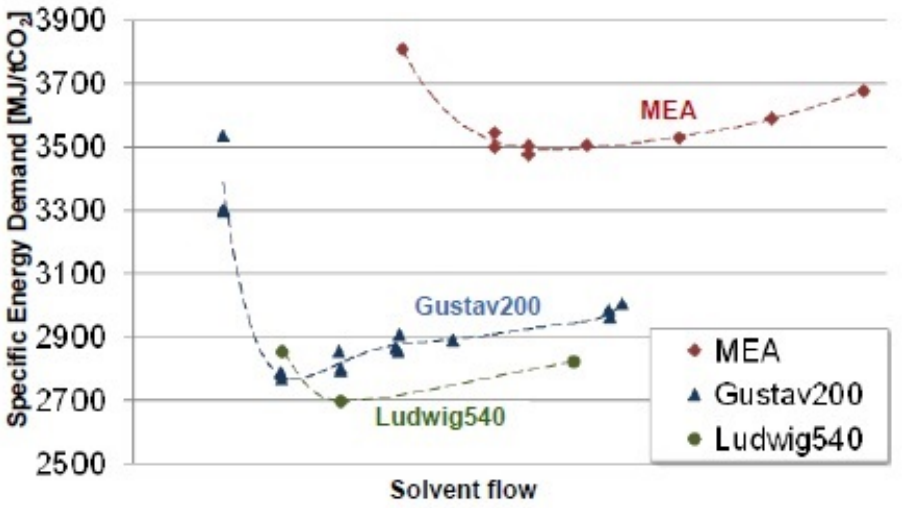

Figure 11. Energy demand for new solvents and an optimized MEA process [59]

One point to be strengthened here is that chemical absorption is also experiencing an intense development in the past time. Some new solvents e.g. Gustav 200 and Ludwig 540 [59] are

synthesized with a lower energy demand (approximate 2700 MJ_{th}/t_{CO2}) for regeneration process, shown in Figure 11.

From the results it is known that if considering the pressure drop in module the counter-current flow shows the best performance in comparison with the other module forms; furthermore, it possesses a better output than the chemical solvents.

5. Conclusions

Membrane technology for gas separation is well suited for the separation of CO_2 from flue gas, *e.g.* in post-combustion capture. Nowadays high performance membrane materials exhibiting a high CO_2 permeability combined with a high CO_2/N_2 selectivity are available. Flat sheet thin film composite membranes are the manufacturing route to transfer the material's superior properties into technical scale membranes realising high fluxes and selectivities simultaneously. Different membrane module concepts are available for this type of membrane. These are spiral wound, envelops type as well as co- and counter-current concepts which were investigated in this study. Pilot plant investigations with synthetic, humidified gas mixtures as well as with power plant flue gas showed a very good performance for the separation of CO_2 using envelope type membrane modules. The pilot plant results could be well represented by process simulation. Assuming that the other module types can be represented equally well, a simulation study was conducted comparing their performance in a virtual pilot plant. It was shown that the differences between the spiral wound, envelope type and four segment counter current module concepts were rather small. A decision for a certain module type based only on simulation results would not be justified. Such a decision should be validated by pilot plant trials for the spiral wound module and counter current concept. Furthermore, investment costs should be put into relation to operational savings. For the one segment co- and counter current module concepts it is

apparent that the long permeate pathways cause disadvantages in operational performance. For the counter current concept the driving force is not applied as efficiently as possible for this flow configuration causing a lower degree of CO_2 separation at essentially the same energy expenditure as for the aforementioned types. For the co-current module this is even more pronounced as the high pressure drop is combined with a disadvantageous flow pattern leading to both, low purity and recovery. This leads in turn to lower compression energies in the vacuum pump and in the recycle compressor. However, it is unlikely that this will offset the inferior performance of the module.

For the scale-up cascaded membrane system simulation the counter current module shows the best performance in comparison with the other module types: the least membrane area and the lowest energy consumption both for 50 and 70% degree of CO_2 separation. A further comparison between the scale-up cascaded membrane system with chemical absorption method shows, that counter current module leads to a better energetic performance.

Acknowledgements

Financial support from the METPORE II project (funding identifier: 03ET2016), funded by the German Minstry of Economics and Energy (BMWi), Germany, within the framework of the COORETEC program, is gratefully acknowledged.

References

1. *World Energy Outlook*, 2012, International Energy Agency.
2. *World Could Be 4 Degrees Hotter By End of This Century, http://www.youtube.com/watch?v=CQbOlI0YQNs&feature=youtu.be*, 2013.
3. *Climate Electricity Annual 2011*, Iternational Energy Agency, http://www.iea.org/publications/freepublications/publication/name,34728,en.html.
4. *Decarbonizing the European Electric Power Sector by 2050: A tale of three studies*, http://cadmus.eui.eu/bitstream/handle/1814/15485/RSCAS_2011_03.pdf?sequence=1.

5. Metz, B., et al., *IPCC Special Report on Carbon Dioxide Capture and Storage*, 2005, Cambridge University Press: United Kingdom & New York, USA, available in full at www.ipcc.ch.
6. *Post-Combustion CO_2 Control*, U.S. Department of Energy, http://www.netl.doe.gov/research/coal/carbon-capture/post-combustion, last access on 16th June, 2014.
7. Kohl, A. and R. Nielsen, *Gas purification 5th ed.*, 1997, Gulf Publishing Company: Houston, Texas.
8. Wang, M., et al., *Post-combustion CO_2 capture with chemical absorption: A state-of-the-art review.* Chem. Eng. Res. Des., 2011. **89**(9): p. 1609-1624.
9. Luis, P., T. Van Gerven, and B. Van der Bruggen, *Recent developments in membrane-based technologies for CO_2 capture.* Progress in Energy and Combustion Science, 2012. **38**(3): p. 419-448.
10. Mangalapally, H.P., et al., *Pilot plant study of four new solvents for post combustion carbon dioxide capture by reactive absorption and comparison to MEA.* Int. J. Greenhouse Gas Control, 2012. **8**: p. 205-216.
11. Svendsen, H.F., E.T. Hessen, and T. Mejdell, *Carbon dioxide capture by absorption, challenges and possibilities.* Chemical Engineering Journal, 2011. **171**(3): p. 718-724.
12. Blomen, E., C. Hendriks, and F. Neele, *Capture technologies: Improvements and Promising Developments.* Energy Procedia, 2009. **1**: p. 1505-1512.
13. Galindo-Cifre, P., et al., *Integration of a chemical process model in a power plant modelling tool for the simulation of an amine based CO_2 scrubber.* Fuel, 2009. **88**(12): p. 2481-2488.
14. Zhao, L., et al., *Multi-stage gas separation membrane processes with post-combustion capture: energetic and economic analyses.* Journal of Membrane Science, 2010. **359**: p. 160-172.
15. Bounaceur, R., et al., *Membrane processes of post-combustion carbon dioxide capture: A parametric study.* Energy, 2006. **31**(14): p. 2220-2234.
16. Favre, E., *Carbon dioxide recovery from post-combustion processes: Can gas permeation membranes compete with absorption?* Journal of Membrane Science, 2007. **294**(1-2): p. 50-59.
17. Car, A., et al., *PEG modified poly(amide-b-ethylene oxide) membranes for CO_2 separation.* Journal of Membrane Science, 2008. **307**(1): p. 88-95.
18. Follmann, P.M., et al., *CO_2 separation via the post-combustion process with membranes in coal power plants*. Efficient Carbon Capture for Coal Power Plants, ed. D. Stolten and V. Scherer2011: Wiley_VCH Verlag GmbH & Co. KGaA. 381-401.
19. Ho, M.T., G.W. Allinson, and D.E. Wiley, *Reducing the Cost of CO_2 Capture from Flue Gases Using Membrane Technology.* Ind. Eng. Chem. Res., 2008. **47**: p. 1562-1568.
20. Deng, L., T.J. Kim, and M.-B. Hägg, *Facilitated transport of CO_2 in novel PVAm/PVA blend membrane.* Journal of Membrane Science, 2009. **340**(1-2): p. 154-163.
21. Hussain, A. and M.-B. Hägg, *A feasibility study of CO_2 capture from flue gas by a facilitated transport membrane.* Journal of Membrane Science, 2010. **359**: p. 140-148.
22. Merkel, T.C., et al., *Power plant post-combustion carbon dioxide capture: An opportunity for membranes.* Journal of Membrane Science, 2010. **359**: p. 126-139.
23. Brinkmann, T., T. Wolff, and J.-R. Pauls. *Post-Combustion Processes Employing Polymeric Membranes*. in *2nd International Conference on Energy Process Engineering Efficient Carbon Capture for Coal Power Plants*. 2011. 20th-22nd, 2011, Frankfurt am Main, Germany.
24. Teruhiko Kai, et al., *Development of commercial-sized dendrimer composite membrane modules for CO_2 removal from flue gas.* Sep. Purif. Technol., 2008. **63**(3): p. 524-530.

25. Powell, C.E. and G.G. Qiao, *Polymeric CO_2/N_2 gas separation membranes for the capture of carbon dioxide from power plant flue gases.* Journal of Membrane Science, 2006. **279**(1-2): p. 1-49.
26. Lin, H. and B. Freeman, *Materials selection guidelines for membranes that remove CO from gas mixtures.* Journal of Molecular Structure, 2005. **739**(1-3): p. 57-74.
27. Reijerkerk, S.R., et al., *Poly(ethylene glycol) and poly(dimethyl siloxane): Combining their advantages into efficient CO2 gas separation membranes.* Journal of Membrane Science, 2010. **352**(1-2): p. 126-135.
28. Brunetti, A., et al., *Membrane technologies for CO_2 separation.* Journal of Membrane Science, 2010. **359**: p. 115-125.
29. Bram, M., et al., *Testing of nanostructured gas separation membranes in the flue gas of a post-combustion power plant.* International Journal of Greenhouse Gas Control, 2011. **5**(1): p. 37-48.
30. Abetz, V., et al., *Developments in Membrane Research: from Material via Process Design to Industrial Application.* Advanced Engineering Materials, 2006. **8**(5): p. 328-358.
31. Sijbesma, H., et al., *Flue gas dehydration using polymer membranes.* Journal of Membrane Science, 2008. **313**: p. 263-276.
32. *MEM-BRAIN Alliance (Gas separation membranes for zero-emission fossil power plants)*, Oct. 2007 - Jun. 2011, 18 research institutions and 5 industrial partners Coordinator: IEF-1, Forschungszentrum Jülich GmbH.
33. *METPORE (Nano-structured Ceramic and Metal Supported Membranes for Gas Separation)*, Jan. 2007 - May. 2014, funded by the Federal Ministry of Economics and Technology (BMWi), Germany.
34. *CO_2 Capture Using Membrane Technology, http://www.nanoglowa.com/.*
35. *The iCap project, http://icapco2.org/empty_11.html.*
36. Car, A., et al., *Tailor-made polymeric membranes based on segmented block copolymers for CO_2 separation.* Advanced Functional Materials, 2008. **18**: p. 2815-2823.
37. Brinkmann, T., et al., *Theoretical and Experimental Investigations of Flat Sheet Membrane Module Types for High Capacity Gas Separation Applications.* Chemie Ingenieur Technik, 2013. **85**(8): p. 1210-1220.
38. Brinkmann, T., et al., *Theoretical and Experimental Investigations of Flat Sheet Membrane Module Types For High Capacity Gas Separation Applications*, in *14th Aachener Membran Kolloquium (AMK)*7^{th}-8^{th} November, 2012: Aachen, Gremany.
39. Brinkmann, T., et al., *Separation of CO_2 from Biogas by Gas Permeation*, in *13th Aachener Membran Kolloquium (AMK)*27^{th}-28^{th} October, 2010: Aachen, Germany.
40. *NETL Greenlights 1 MW Field Test For Membrane Capture Tech, http://ghgnews.com/index.cfm/netl-greenlights-1-mw-field-test-for-membrane-capture-tech/?mobileFormat=false*, 2012.
41. Favre, E., *Polymeric Membranes for Gas Separation*, in *Comprehensive Membrane Science and Engineering*, E. Drioli and L. Giorno, Editors. 2010, Elsevier: UK.
42. Melin, T. and R. Rautenbach, *Membranverfahren*2003: Springer-Verlag, Berlin, 2. Auflage.
43. Baker, R.W., *Membrane Technology and Applications*2012, 3rd Edition: John Wiley & Sons.
44. Ohlrogge, K., J. Wind, and T. Brinkmann, *Membranes for Recovery of Volatile Organic Compounds*, in *Comprehensive Membrane Science and Engineering*, E. Drioli and L. Giorno, Editors. 2010 (Vo. 2), Elsevier: Oxford, UK.
45. Brinkmann, T., *Modellierung und Simulation der Membranverfahren Gaspermeation, Dampfpermeation und Pervaporation*, in *Membranen*, K. Ohlrogge and K. Ebert, Editors. 2006, Wiley-VCH: Weinheim.
46. Car, A., et al., *Pebax/polyethylene glycol blend thin film composite membranes for CO_2 separation.* Separation and Purification Technology, 2008. **62**: p. 110-117.

47. Ohlrogge, K., et al., *Membranverfahren zur Gaspermeation*, in *Membranen*, K. Ohlrogge and K. Ebert, Editors. 2006, Wiley-VCH: Weinheim.
48. *Konzeptstudie: Referenzkraftwerk Nordrhein-Westfalen (RKW NRW), February 2004*, VGB Power Tech e.V., Essen, Germany.
49. *http://www.aspentech.com/products/aspen-custom-modeler.aspx, last access on 27th June 2014*.
50. Metz, S., et al., *Mixed gas water vapor/N transport in poly(ethylene oxide) poly(butylene terephthalate) block copolymers.* Journal of Membrane Science, 2005. **266**(1-2): p. 51-61.
51. Lin, H., et al., *CO_2-selective membranes for hydrogen production and CO2 capture – Part I: Membrane development.* Journal of Membrane Science, 2014. **457**: p. 149-161.
52. Stünkel, S., et al., *Carbon dioxide capture for the oxidative coupling of methane process – A case study in mini-plant scale.* Chemical Engineering Research and Design, 2011. **89**(8): p. 1261-1270.
53. Song, S., et al., *Energy, Equipment and Cost Savings by Using a Membrane Unit in an Amine-Based Absorption Process for CO_2 Removal.* Chemie Ingenieur Technik, 2013. **85**(8): p. 1221-1227.
54. Fang, S.M., S.A. Stern, and H.L. Frisch, *A "free volume" model of permeation of gas and liquid mixtures through polymeric membranes.* Chemical Engineering Science, 1975. **30**(8): p. 773-780.
55. Alpers, A., *Hochdruckpermeation mit selektiven Polymermembranen für die Separation gasförmiger Gemische*, 1997, University of Hannover, PhD Thesis.
56. Ohlrogge, K., J. Wind, and C. Scholles, *Membranverfahren zur Abtrennung organischer Dämpfe in der chemischen und petrochemischen Industrie.* Chemie Ingenieur Technik, 2005. **77**: p. 527-537.
57. Pohlmann, J. and T. Brinkmann, *CO_2 Removal from Power Plant Flue Gases: Gas Permeation Pilot Plant Experiments*, in *15th Aachener Membrane Kolloquium*12th-13th November, 2014, (accepted): Aachen, Germany.
58. Low, B.T., et al., *A parametric study of the impact of membrane materials and process operating conditions on carbon capture from humidified flue gas.* Journal of Membrane Science, 2013. **431**: p. 139-155.
59. Peters, M. and S. Wallus. *Dream Production - Chemical Utilisation of CO_2*. Achema Tagung, Frankfurt am Main June 18, 2012.
60. Zhao, L., M. Weber, and D. Stolten, *Comparative Investigation of Polymer Membranes for Post-combustion Capture.* Energy Procedia, 2013. **37**: p. 1125-1134.
61. Zhao, L., et al., *Cascaded Membrane Processes for Post-Combustion CO_2 Capture.* Chemical Engineering & Technology, 2012. **35**(3): p. 489-496.
62. Zhao, L., et al., *A parametric study of CO_2/N_2 gas separation membrane processes for post-combustion capture.* Journal of Membrane Science, 2008. **325**(1): p. 284-294.
63. Franz, J., et al., *Investigating the influence of sweep gas on CO_2/N_2 membranes for post-combustion capture.* International Journal of Greenhouse Gas Control, 2013. **13**: p. 180-190.